HOKKAIDO UNIVERSITY

Title	A systematic comparison of obsidian hydration measurements : The first application of micro-image with secondary ion mass spectrometry to the prehistoric obsidian
Author(s)	Nakazawa, Yuichi; Kobayashi, Sachio; Yurimoto, Hisayoshi et al.
Citation	Quaternary international, 535, 3-12 https://doi.org/10.1016/j.quaint.2018.05.039
Issue Date	2020-01-10
Doc URL	https://hdl.handle.net/2115/83796
Rights	© 2018. This manuscript version is made available under the CC-BY-NC-ND 4.0 license http://creativecommons.org/licenses/by-nc-nd/4.0/
Rights(URL)	https://creativecommons.org/licenses/by-nc-nd/4.0/
Type	journal article
File Information	QUATINT_2018_96_Revision 1_V0.pdf

Hokkaido University Collection of Scholarly and Academic Papers : HUSCAP

A systematic comparison of obsidian hydration measurements: the first application of micro-image with secondary ion mass spectrometry to the prehistoric obsidian

Yuichi Nakazawa[a,*], Sachio Kobayashi[b], Hisayoshi Yurimoto[c,d], Fumito Akai[e], Hidehiko Nomura[f]

[a] Graduate School of Medicine, Hokkaido University
Kita 15, Nishi 7, Kita-ku, Sapporo, 060-8638, Japan
Phone: +81-11-706-2196
e-mail: ynakazawa@med.hokudai.ac.jp

[b] Kochi Institute for Core Sample Research, Japan Agency for Marine-Earth Science and Technology (JAMSTEC), 200 Monobe-otsu, Nankoku, Kochi 783-8502, Japan

[c] Isotope Imaging Laboratory, Creative Research Institute Sousei, Hokkaido University
Kita 21, Nishi 10, Kita-ku, Sapporo, 001-0021, Japan

[d] Department of Natural History of Science, Hokkaido University
Kita 10, Nishi 8, Kita-ku, Sapporo, 060-0810, Japan

[e] Hokkaido Government Board of Education
Kita 3, Nishi 7, Chuou-ku, Sapporo 060-0003, Japan

[f] Thin Section Laboratory, Group of Technology, Graduate School of Science, Hokkaido University
Kita 10, Nishi 8, Kita-ku, Sapporo, 060-0810, Japan

*Corresponding author

Abstract

Archaeologists have long used obsidian hydration dating method to give chronometric dates for obsidian artifacts. Models using these equations independently employ different measurement systems, which are based on rim thicknesses determined by optical microscope and hydrogen depths measured by secondary ion mass spectrometry (SIMS), respectively, although the inconsistency of both measurements has been reported. Firstly, this paper describes a systematic comparison that was done on optical rim thicknesses and hydrogen depths by means of an isotope microscope, which provides micro-imaging with SIMS. Depth profiles of hydrogen were precisely obtained from the spots where optical measurements were taken on the archaeological obsidian flakes from two distinctive cultural horizons (older: Upper Paleolithic, younger: Initial Jomon) in the stratified open-air site of Jozuka in southern Kyushu (Japan). Secondarily, using the measurements of hydrogen depths that are the most consistent to the measurements of optical thicknesses, the estimated hydration rate of the Holocene (Initial Jomon) is slower than that of the Late Pleistocene (Upper Paleolithic), implying that the difference in hydration rates was due to the difference of intrinsic water content of obsidian and/or obsidian geochemistry. An application of micro-imaging with SIMS to measure hydrogen depths on obsidian shows promise as a tool for improving the practice of hydration dating and evaluating local climatic condition.

Keywords: obsidian; hydration; measurement; secondary ion mass spectrometry; micro-imaging

1. **Introduction**

Because of its easiness of observations, preparations, and availability of samples, archaeologists have used obsidian hydration dating (OHD). Since the earlier stage of the Japanese archaeological studies, OHD has been employed for constructing cultural chronologies (e.g., Suzuki 1971; Katsui and Kondo, 1976, see also Nakazawa, 2015). However, a rapid progress of tephrochronology since the 1970's has given general framework to allow to create regional chronologies of the Japanese prehistoric sites (e.g., Moriwaki et al., 2016), and this made archaeologists less relied on chronometric method to temporal significance on the archaeologically constructed unit (e.g., site, assemblage, artifact). Contrary, a progress of Paleolithic research over the last 70 years now gives rich but complex picture of Japanese Paleolithic archaeological record (Kaifu et al., 2015; Nakazawa, 2011, 2017), which further requires to explore reliable chronometric dating methods to understand Paleolithic in East Asia. Under this circumstance, use of ^{14}C dates has now become critical to give dates for the sites and assemblages to help to support various chronologies of the Japanese prehistory (e.g., Ono et al., 2002; Shoda, 2010; Nakazawa et al., 2011; Izuho and Kaifu, 2015; Morisaki and Natsuki, 2017). However, chronometric dates notably ^{14}C dates are not always available from archaeological sites and their reliability needs to be assessed by other methods. Moreover, given intensive exploitations of obsidian by the prehistoric populations lived in the Japanese Archipelago, it is worthwhile to explore the OHD for an alternative method.

Obsidian hydration has known as the diffusion of ambient water into a glass matrix of obsidian forms a hydration rim that is the function of the time elapsed since the fresh surface of obsidian has been exposed. The relationship between elapsed time and

71 thickness of the hydration rim on an obsidian flake gives the theoretical basis for the
72 OHD. The traditional method for measuring hydration rim thickness is based on the
73 optical principle that a microscopically observed hydrated layer appears due to the flux
74 of light (Friedman and Smith, 1960). However, the optical method of measurements has
75 been challenged by the new diffusion model explicating that the diffusion of molecular
76 water into a glass solid is dependent on the concentration of intrinsic water in the
77 obsidian (Anovitz et al., 1999; Liritzis, 2006; Novak and Stevenson, 2012; Rogers,
78 2008; Stevenson and Novak, 2011, see also Ambrose, 1976; Haller, 1963, Lee et al.,
79 1974). In the new diffusion model, the depth profiles of the hydrogen on the hydrated
80 obsidian surfaces diagnosed by the secondary ion mass spectrometry (SIMS) offer a
81 critical method for evaluating variations in diffused water (e.g., Anovitz et al., 1999,
82 2004, 2006a, 2006b; Liritzis 2006; Liritzis and Laskaris, 2011; Riciputi et al., 2002;
83 Steffen, 2005; Stevenson et al., 2001, 2004). Because currently two measurement
84 systems are being used, an explicit comparison of the depth profiles of hydrogen and the
85 optical rim thicknesses is necessary if we are to discuss how the two measurement
86 systems are integrated. The primary goal of this paper is to make an explicit comparison
87 of the optically measured hydration rim thickness and depth of hydrogen precisely
88 assessed by the isotope microscope that equipped SIMS to create micro-images of
89 hydrogen profiles (Yurimoto et al., 2003). The second goal is to give a gross estimate of
90 the Pleistocene hydration rate that may be useful for evaluating paleoclimatic regimes.
91

92 **2. An application of the secondary ion mass spectrometry (SIMS) to obsidian**
93 **hydration dating method**

94 At present, both traditional and new diffusion models have been employed in

obtaining obsidian hydration equations. For the traditional model, empirically developed quadratic equation has yielded dates based on the optically measured thickness of the hydration rim and time (Friedman and Smith, 1960; Friedman and Long, 1976). The equation is $x^2 = kt$

where x = rim thickness (μm), t = time, and k = diffusion rate.

In the quadratic equation, the thickness of the hydration rims created by stress birefringence in the optical principle (Anovitz et al., 1999; Michels et al., 1983; Liritzis, 2014) is measured under the polarized microscope (Friedman and Smith, 1960). Although the quadratic equation does not provide the best solution for some archaeological dates (e.g., Ridings, 1996; Riciputi et al., 2002), with refining the estimation of the effective hydration temperature (Rogers, 2007), the considerations of chemical difference (Suzuki, 1971; Friedman and Smith, 1976; Hughes, 1988; Watanabe and Suzuki, 2005; Behrens and Zhang, 2009), and the effect of the intrinsic water content of the obsidian (Ambrose, 1976; Stevenson et al., 1993, 1998; Steffen, 2005; Rogers, 2008, 2013; Rogers and Duke, 2011), the traditional model has been continuously improved to address various archaeological research questions (e.g., Ambrose, 1993; Hull, 2001; Dillian, 2002; Eerkens et al., 2008; Nakazawa, 2015; Tripcevich et al., 2012).

On the other hand, the new model that provides the concentration-dependent diffusion equation based on Fick's second diffusion law is, described as $\partial C/\partial t = \partial/\partial x(D\partial C/\partial x)$

where C is the concentration of hydrogen, x is the depth of hydrogen, t is the time, and D is the diffusion coefficient (Anovitz et al., 1999; Riciputi et al., 2002; Liritzis, 2014). The concentration-dependent diffusion equation describes the diffusion of water

119 molecule from the exposed surface to the inward unhydrated glass matrix. When the
120 effective hydration temperature is constant, the rate of diffusion is largely dependent on
121 the variability in the intrinsic water content (e.g., Anovitz et al., 1999; Delaney and
122 Karsten, 1981; Haller, 1963; Zhang et al., 1997; Stevenson et al., 1998; Riciputi et al.,
123 2002; Rogers, 2008; Behrens and Zang, 2009).
124 Since the proposal of a new diffusion model, the estimated concentration-dependent
125 diffusion coefficient has been established often by SIMS in order to give an accurate
126 hydration date (e.g., Anovitz et al., 1999; Liritzis, 2014; Riciputi et al., 2002). The
127 fundamental reason to explore the SIMS profile readings for the depth of hydrogen in
128 the new diffusion model is that it has great potential for understanding the surface
129 dynamics of molecular water into glass (Anovitz et al., 1999, 2004, 2008; Liritzis and
130 Diakostamatiou, 2002; Stevenson et al., 2004). Depth profiles of hydrogen on obsidian
131 surfaces exhibits S-shaped (precisely it is a mirror image of S) curve, but they do not
132 necessarily correspond to the optical boundary between the hydrated obsidian surface
133 and the obsidian without hydration, thus weakening the reliability of the optical
134 measurements in using the traditional model to give dates (Anovitz et al., 1999; Riciputi
135 et al., 2002). While SIMS serves as a critical method for applying a new diffusion
136 model to OHD, taking measurements of the depth of the diffused water molecules from
137 the surface on a SIMS profile is not straightforward because the diffusion front shows a
138 gradual decrease of hydrogen. Moreover, even in the equations that estimate diffusion
139 coefficient based on gradient water profiles (Liritzis, 2006; Liritzis and Diakostamatiou,
140 2002; Riciputi et al., 2002), the depths of the water molecules are a prerequisite for
141 computing hydration dates. Given the current situation in which both traditional and
142 new diffusion models with corresponding analytical methods (i.e., optical microscopic

measurements and SIMS profiling) are juxtapose, the present study introduces the micro-imaging with SIMS, a new method of measurement that can bridge the two measurement methods.

3. Materials and methods

3-1. Samples from two temporal units at a single site of Jozuka, southern Kyushu, Japan

The study site is from southern Kyushu, a large island south of the Korean Peninsula and east of the southern China across the Tsushima Strait and the East China Sea, respectively (Fig. 1). Despite the fact that the archaeological sites in southern Kyushu have yielded abundant obsidian artifacts from the well-stratified open-air sites often blanketed by a series of the Late Pleistocene and Holocene tephra units, OHD has not been used for dating archaeological assemblages. Samples of obsidian artifacts for the present study were obtained from the two assemblages with reliable dates in the identical archaeological site of Jozuka (31° 36’40’’N, 130°57’30’’E) (Fig. 1). Jozuka is an open-air site characterized by multiple occupational levels from the Late Pleistocene to Holocene (Kagoshima Prefectural Archaeological Center, 2010). Artifacts and features were encompassed in the aeolian loam blanketed by multiple tephra layers that have known erupted dates. A total of three cultural horizons (i.e., Final Jomon, Initial Jomon, and Upper Paleolithic) were identified in the sequentially ordered lithostratigraphic units (Fig. 2). Because vertical separation of three cultural horizons is distinctive and no significant evidence of anthropogenic and natural disturbances is identified (Kagoshima Prefectural Archaeological Center, 2010), inter-stratigraphic mixture of artifacts between different cultural horizons is unlikely.

Study samples were obtained from two occupational levels: Level XVI, which is

167 culturally affiliated to the early Upper Paleolithic, and Level VII, the Initial Jomon
168 period, a cultural period characterized by a subsistence economy based on hunting,
169 gathering, and fishing assisted by the use of pottery (Kagoshima Prefectural
170 Archaeological Center, 2010). Although, no chronometric dates were obtained from the
171 lower levels at the Jozuka site, the bottom layer (Level XVIII) of the site has a marker
172 tephra of AT, erupted at 30,000 cal. B.P. (Miyairi et al., 2004; Yokoyama et al., 2007;
173 Smith et al., 2013), and Level XVI encompasses the tephra called P17, erupted ca.
174 26,000 cal. B.P. (Okuno, 2002) from the local volcano of Sakurajima, 30 km west of the
175 study site of Jozuka (Fig. 1). In contrast, Level VII characterized by dense human
176 occupations during the Initial Jomon has a total of 14 radiocarbon dates that were
177 obtained from organic stains on pottery and features including pits, pit-houses, and
178 stone heaps consisting of fire-cracked rocks (Table 1). Represented by the median date
179 among the total of 14 radiocarbon dates obtained from the features in Levels VII and
180 VIII, we treated 10,500 cal. B.P. as the date of the Initial Jomon occupation. Thus, two
181 sets of obsidian samples were from human occupations that are 15,500 years apart.
182 Because the temporally different samples are from the identical site, differences in the
183 thermal histories between the two assemblages would be caused by soil temperatures
184 that varied depending on the duration of artifacts' depositions (Jones et al., 1997;
185 Ridings, 1991).
186 The optical measurements of the hydration rims were conducted under a polarized
187 microscope (MT9300, Meiji Techno Co., LTD.) at the magnifications of 400×. Three
188 measurements both on exterior (dorsal) and interior (ventral) surfaces of a single
189 obsidian flake sample were recorded at the μm using the computer-assisted measuring
190 devise (Art Measure, Artray Inc.). Observations and measurements on obsidian

191 hydration were exclusively conducted by the first author, nullified the inter-observer
192 errors. After taking pictures of all measured spots on the rims, all SIMS profiles were
193 taken within 140 μm range around the exact spots where the optical measurements were
194 done (Fig. 3). Among the sampled obsidian flakes, thicknesses were all measured by
195 optical microscope: three samples from the younger occupation and three samples from
196 the older occupation at the study site of Jozuka were chosen for the SIMS analysis. A
197 total of 13 SIMS profiles comprised of six measurements from the younger samples and
198 seven measurements from the older samples were taken. To increase the efficiency in
199 taking SIMS measurements, all samples were sliced into small pieces to embed them
200 into a columnar epoxy.
201
202 *3-2. Hydrogen imaging and secondary ion-mass spectrometry*
203 Previous applications of SIMS on the hydrated surfaces of obsidian have
204 demonstrated that hydrogen profiles are characterized by the S-shaped profile of water
205 concentration as the function of depth. As Anovitz et al. (1999: 739) describes,
206 concentration-dependent S-shaped profile has a typical pattern: first, water
207 concentrations are initially flat or decrease slowly. Second, water concentration
208 decreases rapidly. Third, water concentration decreases slowly into the background (see
209 also Lirtzis 2006; Riciputi et al., 2002). However, it has not fully evaluated the extent to
210 which the optical method of hydration measurements is reliable with respect to the
211 measured hydrogen depth by SIMS. An earlier observation of hydrogen profiles of
212 archaeological obsidian artifacts suggests that optically measured hydration rim
213 thicknesses do not correspond to the depths of hydrogen (Anovitz et al., 1999). A more
214 systematic comparison has demonstrated that optical measurements systematically

overestimate hydrogen depths (Riciputi et al., 2002: 1069; Stevenson et al., 2004: 564). In contrast, the other comparisons have shown that the optical measurements the underestimate hydrogen depths despite their correlation (Novak and Stevenson, 2012: 8-9; Stevenson et al., 2001: 112-113). Given an additional observation that the difference between the optical measurements and hydrogen depths becomes larger as the optical measurements increase, Stevenson et al. (2001: 114) notes that an optical boundary (i.e., Becke line [Anovitz et al., 1999: 744]) was observed at a point shallower than the actual diffusion front because a hydrogen profile becomes flat "within the region of the hydration rim diffusion front." The current uncertainty of correspondence between optical and hydrogen profiles are not only because of the difference in principles and models, but also because the spots where the measurements were taken were uncontrollable. Even though we have known that optically measured hydration thicknesses are often varied in a single specimen (e.g., Origer, 1989; Dillian, 2002; Nakazawa, 2015), current SIMS measurements are either better applied to a relatively flat surface (e.g., Liritzis and Laskaris, 2012; Novak and Stevenson, 2012) or to anonymous locations in a given specimen (e.g., Anovitz et al., 1999; Stevenson et al., 2004; Liritzis, 2014) that do not necessarily correspond to the spots where the optical measurements were taken. Thus, the reliability of the two methods needs to be evaluated by taking two kinds of measurements at an identical spot within a single hydration rim.

To obtain accurate hydrogen profiles, here, we used an isotope microscope in which the Cameca ims-1270 is equipped with Stacked CMOS-type Active Pixel Sensor (Yurimoto et al. 2003). The sample surface was homogeneously irradiated over a field area of diameter ~100 μm, using a broad O^- primary beam set to 23 keV and 20 nA.

Stigmatic images of the positive secondary ions of $^{1}H^{+}$ and $^{28}Si^{+}$ were acquired in each analyzed area. The exposure time was typically 500 s for $^{1}H^{+}$ and 10 s for $^{28}Si^{+}$. The lateral resolutions of the secondary ion images were ~0.5 μm using a contrast aperture of 50 μm in diameter. The isotope microscope is specifically designed to make micro-scale images from quantified elements by SIMS (e.g., Yurimoto and Nagashima, 2005; Kawasaki et al., 2012). In the present study, it enables us to capture elements on hydrated and unhydrated surface at the same spot where an optical measurement has been taken. The depth of the hydrogen is delimited in accordance with the imaged hydrogen concentration at the micro scale. The hydration concentration is clearly visible as a bright band in the micro-image (Fig. 4a). In Fig 4a, x is the point on the surface of obsidian and the perpendicular line that transects x on the diminishing margin of bright band is regarded as y, the hydration front. Then, the measured distance between x and y based on the micro-image in Fig. 4a gives the profile of the hydration concentration delimited by x and y (Fig. 4b). Profiles of the elements of interests (e.g., H, Si) can be repeatedly created along any of the lines on the images, using the image analysis program Image J2 (free software available at http://imagej.net/ImageJ2). These functions allow us to make an explicit comparison of hydrogen profiles and optical measurements.

4. Results and discussion

Thicknesses of the hydration rims and hydrogen depths compared among the 13 spots that were measured (Table 2, Fig. 5). Although measurement errors can be involved both for optical method and SIMS, because of its high precision the measured hydrogen depths would be less involved errors than the optical rim thicknesses. Thus, here we

263 treat that the hydrogen depths as the independent variable and the optical rim
264 thicknesses as the dependent variable. Although a systematic difference between the
265 optical rim thicknesses and hydrogen depths has been reported by Riciputi et al. (2002)
266 and Stevenson et al. (2004), the plots of measurements in Figure 5 are more or less
267 equally placed over and under the regression spline, while the specimens from the
268 Upper Paleolithic level (Level XVI) are generally closer to the regression line than
269 those from the Initial Jomon level (Levels VII, and VIII). This visual observation is
270 further examined by linear regression analysis. Using the regression equation for the
271 present sets of measurements: $Y = 2.155 + 0.713X$, the predicted rim thicknesses and
272 raw residuals (d_{Y*X}) are calculated (Table 2, see VanPool and Leonard, 2011),
273 where Y = rim thickness, X = hydrogen depth, $d_{Y*X} = Y_i - \hat{Y}$. Based on the raw residuals,
274 the optical thicknesses for the specimens of Upper Paleolithic are thicker than the
275 expected based on the hydrogen depths, suggesting that optical measurements
276 overestimated the hydrogen depths. In contrast, the optical measurements for the
277 specimens of Initial Jomon were thinner than the hydrogen depths, implying the optical
278 measurements underestimated the hydrogen depths.
279 Because the hydration rate of obsidian was sensitively varied depending on
280 temperature (Friedman and Long, 1976; Rogers, 2007), it is generally expected that
281 hydration rate for the Holocene is faster than the Pleistocene. Temperature history is
282 expected to be spatially unvaried at the study site of Jozuka because it is a single open-
283 air site with multiple occupational levels from the Late Pleistocene to the Holocene
284 (Upper Paleolithic to Jomon). Taking this advantage, here we give a gross estimation of
285 hydration rate for the Late Pleistocene in the southern Kyushu through an assessment of
286 the difference in the hydration rates between the Pleistocene and Holocene. An analysis

of standardized residuals (VanPool and Leonard, 2011: 211-213) is performed to extract the representative measurements to estimate the hydration rates (Table 2).

Because the standard residuals of the measurements from J-2445-v-1 and J-8641-d-2 are less variable than the other samples (Table 2), these two measurements are legitimately employed for estimating the Late Pleistocene and Holocene hydration rates of obsidian. Using the SIMS measurement of hydrogen depth for the Upper Paleoithic specimen J-2445-v-1 that retains the most consistent measurement between the optical hydration rim thickness and hydrogen depth, the hydration date is estimated by the equation: $x^2 = kt$. For the J-2445-v-1,

$k_{UP} = x_{UP}{}^2 / t_{UP}$

$= (12.89)^2 / 26000$

$= 0.006390$

$= 6.39 \times 10^{-3}$

where $x_{UP} = 12.89$ (μm) and $t_{UP} = 26000$ (years ago).

Thus, the hydration rate for the specimens of Upper Paleolithic level of the Jozuka site, southern Kyushu is 6.39 μm per 1000 years. This hydration rate is the averaged during the last 26,000 years of deposition, which encompasses both the Late Pleistocene and Holocene. What we are interested in, however, is the difference in hydration rates for the Late Pleistocene and Holocene. This requires us to isolate the Late Pleistocene hydration rate through an assessment of the Holocene hydration rate.

A hydration rate for the Holocene is estimated from the specimen of the Initial Jomon (10,500 years ago). Because of its proximity of measurements between microscopic thickness and hydrogen depth (Table 2), the measurement of J-8641-d-2 is used for an estimation of Holocene hydration rate. For the J-8641-d-2,

311 $k_J = x_J^2 / t_J$

312 $= (6.53)^2 / 10500$

313 $= 0.004061$

314 $= 4.061 \times 10^{-3}$

315 where $x_J = 6.53$ (μm) and $t_J = 10500$ (years ago).

316 Because the Holocene temperature is higher than the Pleistocene, it is expected that k_J
317 is faster than k_{UP}. Contrary to this expectation, as shown above, k_{UP} estimated from
318 Upper Paleoltihic specimen (J-2445) is faster than k_J using the Initial Jomon specimen
319 (J-8641). This contradictory result can be explained by factors other than thermal
320 histories, such as intrinsic water content (Ambrose, 1976) and geochemistry of obsidian
321 (Suzuki, 1971). Because this is the pilot study, we have not performed geochemical
322 analysis and measuring water content for the specimens. A study of geochemical
323 analysis for the obsidian outcrops in southern Kyushu has distinguished a total of 10
324 sources (Mukai, 2008), suggesting that the obsidian specimens for the present study
325 might be from multiple sources. Because the different obsidian sources have different
326 diffusion rate (e.g., Michels et al., 1983; Watanabe and Suzuki, 2006), the slower rate of
327 hydration for the Initial Jomon specimen (J-8641) and the faster rate of hydration for the
328 Upper Paleolithic specimen (J-2445) could be due to the differences in intrinsic water
329 content (Stevenson et al., 1993) and obsidian geochemistry. This needs to be
330 investigated in the future research.

331 In the traditional model of OHD, k is a critical variable. In estimating k, temperature
332 is given as time-averaged. While the global climatic records have shown the
333 millennium-scale fluctuations of climatic changes (e.g., Yuan et al., 2004), the local
334 climatic fluctuations would have been more effective to human behavior than the global

climatic changes (e.g., Nakazawa et al., 2011; Iizika and Izuho, 2017). In this sense, besides rigorous experimental approach (e.g., Anovitz et al., 2006a), an examination of hydration rate through an application of the traditional model of OHD to empirical archaeological data is also worthwhile to evaluate local climatic condition, particularly paleo-temperature regime.

5. Conclusion

The present study compared the measurements between optical rim thicknesses and hydrogen depths by taking an advantage of the isotope microscope that gives distinctive micro-images of hydrogen profiles at the exact spots where optical measurements were taken. This method not only increases the reliability of measurements, but also makes a deeper profile (> 10 μm) based on a high spatter rate lessen the duration of analysis. The systematic comparison of two kinds of measurements showed good correlation, implying that micro-imaging with SIMS is useful method to evaluate the extent to which the optical measurements are reliable. Using the reliable measurements assessed by the micro-imaging with SIMS, the estimated hydration rate can be validly evaluated. Imaging diffused hydrogen concentration on the surface of an archaeological obsidian artifact is an emerging methodological approach that will open new research avenues, therein improving the practice of OHD.

Acknowledgements

The samples of obsidian artifacts used for the present study were obtained under the permission of the Kagoshima Prefectural Archaeological Center. We thank Ryoichi Maesako, Koji Okubo, Akie Seki, and Aya Manabe for their help in the sampling

processes. We are also grateful to Thomas Origer, Janine Loyd, Masami Izuho, and Dr. Jinichiro Maeda for their generous help and advice. We thank Dr. Naoya Sakamoto for his professional assistance in sample preparation for SIMS. Constructive comments from two anonymous reviewers helped to revise the manuscript. The present study was supported by JSPS KAKENHI Grant Number 26350374, and partly supported by the "Cultural history of PaleoAsia: Integrative research on the formative processes of modern human cultures in Asia," directed by Yoshihiro Nishiaki (The University of Tokyo) and funded by the Grant-in-Aid for Scientific Research on Innovative Areas (Grant No. 1802 for FY2016–2020) from the Ministry of Education, Culture, Sports, Science and Technology, Japan.

370 **References Cited**

371 Ambrose, W., 1976. Intrinsic hydration rate dating of obsidian. In: In Taylor, R.E. (Ed.),
372 Advances in Obsidian Glass Studies. Noyes Press, Park Ridge, NJ, pp. 81-105.
373 Ambrose, W., 1993. Obsidian hydration dating. In: Fankhauser, B.L., Roger Bird, J.
374 (Eds.), Archaeometry: Current Australasian Research. The Australian National
375 University, Canberra, pp. 79-84.
376 Anovitz, L.M., Elam, J.M., Riciputi, L.R., Cole, D.R., 1999. The failure of obsidian
377 hydration dating: sources, implications, and new directions. J. Archaeol. Sci. 26, 735-
378 752.
379 Anovitz, L.M., Elam, J.M., Riciputi, L.R., Cole, D.R., 2004. Isothermal time-series
380 determination of the rate of diffusion of water in Pachuca obsidian. Archaeometry 46,
381 301-326.
382 Anovitz, L.M., Riciputi, L.R., Cole, D.R., Fayek, M., Elam, J.M., 2006a. Obsidian
383 hydration: a new paleothermometer. Geology, 34-7, 517-520.
384 Anovitz, L.M., Riciputi, L.R., Cole, D.R., Gruszkiewicz, M.S., Elam, J.M., 2006b. The
385 effect of changes in relative humidity on the hydration rate of Pechuca obsidian. J. Non-
386 Cryst. Solids, 352, 5652-5662.
387 Anovitz, L.M., Cole, D.R., Fayek, M., 2008. Mechanisms of rhyolitic glass hydration
388 below the glass transition. Am. Mineral., 93, 1166-1178.
389 Behrens, H., Zhang, Y., 2009. H_2O diffusion peralkaline to peraluminous rhyolitic
390 melts. Contrib. to Mineral. Petrol. 157, 765-780.
391 Delaney, J.R., Karsten, J.L., 1981. Ion microprobe studies of water in silicate melts:
392 concentration-dependent water diffusion in obsidian. Earth and Planet. Sci. Lett., 52,
393 191-202.

394 Dillian, C. D., 2002. More than Toolstone: Differential Utilization of Glass Mountain
395 Obsidian. Unpublished Ph.D. dissertation. University of California, Berkeley.
396 Doremus, R.H., 2000. Diffusion of water in rhyolite glass: diffusion-reaction model. J.
397 Non-Cryst. Solids, 261, 101-107.
398 Eerkens, J.W., Vaughn, K., Carpenter, T.R., Conlee, C.A., Linares Grados, M.,
399 Schreiber, K., 2008. Obsidian hydration dating on the South Coast of Peru. J. Archaeol.
400 Sci. 35, 2231-2239.
401 Friedman, I., Long, W., 1976. Hydration rate of obsidian. Science 191, 347-352.
402 Friedman, I., Smith, R.L., 1960. A new dating method using obsidian: part I, the
403 development of the method. Am. Antiq. 25, 476-493.
404 Haller, W., 1963. Concetration-dependent diffusion coefficient of water in glass. Phys.
405 Chem. Glasses 4, 217-220.
406 Hughes, R.E., 1988. The Coso volcanic filed reexamined: implications for obsidian
407 sourcing and hydration dating research. Geoarchaeology 3, 253-265.
408 Hull, K.L., 2001. Reasserting the utility of obsidian hydration dating: a temperature-
409 dependent empirical approach to practical temporal resolution with archaeological
410 obsidians. J. Archaeol. Sci. 28, 1025-1040.
411 Iizuka, F., and Izuho, M., 2017. Late Upper Paleolithic-Initial Jomon transitions,
412 southern Kyushu, Japan: regional scale to macro processes a close look. Quaternary
413 International 441, 102-112.
414 Izuho, M., Kaifu, Y., 2015. The appearance and characteristics of the Early Upper
415 Paleolithic in the Japanese Archipelago. In: Kaifu, Y., Izuho, M., Goebel, T., Sato, H.,
416 Ono, A., (Eds.), Emergence and Diversity of Modern Human Behavior in Paleolithic
417 Asia, Texas A&M Press, College Station, pp. 289-313.

418 Jones, M., Sheppard, P.J., Sutton, D.G., 1997. Soil temperature and obsidian hydration
419 dating: a clarification of variables affecting accuracy. J. Archaeol. Sci. 24, 505-516.
420 Kagoshima Prefectural Archaeological Center, 2010. Jozuka Site/Inamura Site,
421 Kagoshima Prefectural Archaeological Center, Kirishima City. (in Japanese)
422 Kaifu, Y., Izuho, M., Goebel, T., 2015. Modern human dispersal and behavior in
423 Paleolithic Asia. In: Kaifu, Y., Izuho, M., Goebel, T., Sato, H., Ono, A., (Eds.),
424 Emergence and Diversity of Modern Human Behavior in Paleolithic Asia, Texas A&M
425 Press, College Station, pp. 535-566.
426 Katsui, Y., Kondo, Y., 1976. Variation in obsidian hydration rates for Hokkaido,
427 northern Japan. In: Taylor, R.E. (Ed.), Advances in Obsidian Glass Studies. Noyes
428 Press, Park Ridge, NJ, pp. 120e140.
429 Kawasaki, N., Sakamoto, N., Yurimoto, H., 2012. Oxygen isotopic and chemical zoning
430 of melilite crystals in a type A Ca-Al-rich inclusion of Efremovka CV3 chondrite.
431 Meteorit. Planet. Sci. 47, 2084-2093.
432 Lee, R.R., Ericson, J.E., Friedman, I., 1974. Obsidian hydration profile measurements
433 using a nuclear reaction technique. Nature 250, 44-47.
434 Liritzis, I., 2006. SIMS-SS, a new obsidian hydration dating method: analysis and
435 theoretical principles. Archaeometry 48, 533-547.
436 Liritzis, I., 2014. Obsidian hydration dating. In: Rink, W.J., Thompson, J.W., (Eds.)
437 Encyclopedia of Scientific Dating Methods. Springer, pp. 1-23.
438 Liritzis, I., Diakostamatiou, M., 2002. Towards a new method of obsidian hydration
439 dating with secondary ion mass spectrometry via a surface saturation layer approach.
440 Medit. Archaeol. and Archaeometry, 2, 3-20.
441 Liritzis, I., Laskaris, N., 2011. Fifty years of obsidian hydration dating in archaeology.

J. Non-Cryst. Solids, 357, 2011-2023.

Liritzis, I. and Laskaris, N., 2012. The SIMS-SS obsidian hydration dating method. In: Liritzis, I., Stevenson, C.M., (Eds.) Obsidian and Ancient Manufactured Glasses. University of New Mexico Press, Albuquerque, pp. 26-45.

Mazer, J.J., Bates, J.K., Stevenson, C.M., Bradley, C.R., 1992. Obsidian and tektites: natural analogues for water diffusion in nuclear waste glasses. Materials Research Society Symposium Proceedings 257, 513-520.

Michels, J.W., Tsong, I.S.T., Nelson, C.M., 1983. Obsidian dating and East African archaeology. Science, 219, 361-366.

Miyairi, Y., Yoshida, K., Miyazaki, Y., Matsuzaki, H., Kaneoka, I., 2004. Improved ^{14}C dating of a tephra layer (AT tephra, Japan) using AMS on selected organic fractions. Nucl. Instr. Meth. Phys. Res. B 223-224, 555-559.

Moriwaki, H., Nakamura, N., Nagasako, T., Lowe, D.J., Sangawa, T., 2016. The role of tephras in developing a high-precision chronostratigraphy for palaeoenvironmental reconstruction and archaeology in southern Kyushu, Japan, since 30,000 cal. BP: an integration. Quaternary International 397, 79-92.

Morisaki, K., Natsuki, D., 2017. Human behavioral change and the distributional dynamics of early Japanese pottery. Quaternary International 441, 91-101.

Mukai, M., 2008. Chemical compositions of the obsidian glasses produced from South Kyushu. Bulletin of the Asahikawa City Museum 14, 1-30. (in Japanese)

Nakazawa, Y., 2010. Dual nature in the creation of disciplinary identity: a socio-historical review of Palaeolithic archaeology in Japan. Asian Perspectives 49, 231-250.

Nakazawa, Y., 2015. The significance of obsidian hydration dating in assessing the integrity of Holocene midden, Hokkaido, northern Japan. Quat. Int. 397, 474-483.

466 Nakazawa, Y., 2017. On the Pleistocene population history in the Japanese
467 Archipelago. Current Anthropology 58, Supplement 17, S539-S552.
468 Nakazawa, Y., Iwase, A., Akai, F., Izuho, M., 2011. Human responses to the Younger
469 Dryas in Japan. Quaternary International 242, 416-433.
470 Novak, S.W., Stevenson, C.M., 2012. Aspects of secondary ion mass spectrometry
471 (SIMS) depth profiling for obsidian hydration dating. In: Liritzis, I., Stevenson, C.M.,
472 (Eds.) Obsidian and Ancient Manufactured Glasses. University of New Mexico Press,
473 Albuquerque, pp. 3-14.
474 Okuno, M., 2002. Chronology of tephra layers in southern Kyushu, SW Japan, for the
475 Last 30,000 years. The Quat. Res. (Daiyonki-Kenkyu), 41, 225-236.
476 Ono, A., Sato, H., Tsutsumi, T., Kudo, Y., 2002. Radiocarbon dates and archaeology of
477 the Late Pleistocene in the Japanese Islands. Radiocarbon 44, 477-494.
478 Origer, T.M., 1989. Hydration analysis of obsidian flakes produced by Ishi during the
479 historic period. Contrib. Univ. California Archaeol. Res. Facil. 48, 69-77.
480 Riciputi, L.R., Elam, J.M., Anovitz, L.M., Cole, D.R., 2002. Obsidian diffusion dating
481 by secondary ion mass spectrometry: a test using results from Mound 65, Chalco,
482 Mexico. J. Archaeol. Sci. 29, 1055-1075.
483 Ridings, R., 1991. Obsidian hydration dating: the effects of mean exponential ground
484 temperature and depth of artifact recovery. J. Field Archaeol. 18, 77-85.
485 Ridings, R., 1996. Where in the world does obsidian hydration dating work?
486 American Antiquity 61, 136-148.
487 Rogers, A.K., 2007. Effective hydration temperature of obsidian: a diffusion theory
488 analysis of time-dependent hydration rates. J. Archaeol. Sci. 34, 656-665.
489 Rogers, A.K., 2008. Obsidian hydration dating: accuracy and resolution limitations

490 imposed by intrinsic water variability. J. Archaeol. Sci. 35, 2009-2016.
491 Rogers, A.K., 2013. Intrinsic water in obsidian and its effect on hydration rate: a case
492 study from the Coso volcanic field, Inyo County, California. Int. Assoc. of Obsidian
493 Stud. Bull., 17-22.
494 Rogers, A.K., Duke, D., 2011. An archaeologically validated protocol for computing
495 obsidian hydration rates from laboratory data. J. Archaeol. Sci. 38, 1340-1345.
496 Schmidt, B.C., Blum-Oeste, N., Flagmeier, J., 2013. Water diffusion in phonolite melts.
497 Geochem. Cosmochim. Acta 107, 220-230.
498 Shoda, S., 2012. Radiocarbon and archeology in Japan and Korea: what has changed
499 because of the Yayoi dating controversy? Radiocarbon 52, 421-427.
500 Smith, V.C., Staff, R.A., Blockley, S.P.E., Bronk-Ramsey, E., Nakagawa, T., Mark,
501 D.F., Takemura, K., Danhara, T., Suigetsu 2006 Project Members, 2013. Identification
502 and correlation of visible tephras in the Lake Suigtetsu SG06 sedimentary archive,
503 Japan: chronostratigraphic markers for synchronizing of east Asian/west Pacific
504 palaeoclimatic records across the last 150 ka. Quat. Sci. Revs. 67, 121-137.
505 Steffen, A. 2005. The Dome Fire Obsidian Study: Investigating the Interaction of Heat,
506 Hydration, and Glass Geochemistry. Unpublished Ph.D. dissertation. University of New
507 Mexico, Albuquerque.
508 Stevenson, C.M., Knauss, E., Mazer, J.J., Bates, J.K., 1993. Homogeneity of water
509 content in obsidian from the Coso volcanic field: implications for obsidian hydration
510 dating. Geoarchaeology 8, 371-384.
511 Stevenson, C.M., Mazer, J.J., Scheetz, B.E., 1998. Laboratory obsidian hydration rates:
512 theory, method, and application. In: Shackley, M.S. (Ed.), Archaeological Obsidian
513 Studies. Plenum Press, New York, pp. 181-204.

514 Stevenson, C.M., Abdelrehim, I.M., Novak, S.W., 2001. Infra-red photoacaustic and
515 secondary ion mass spectrometry measurements of obsidian hydration rims. J. Archaeol.
516 Sci. 28, 109-115.
517 Stevenson, C.M., Abdelrehim, I, Novak, S.W., 2004. High precision measurement of
518 obsidian hydration layers on artifacts from the Hopewell site using secondary ion mass
519 spectrometry. Am. Antiq. 69, 555-568.
520 Stevenson, C.M., Novak, S.W., 2004. Obsidian hydration dating by infrared
521 spectroscopy: method and calibration. J. Archaeol. Sci. 38, 1716-1726.
522 Suzuki, M., 1971. Chronology of prehistoric human activity in Kanto, Japan, Part I:
523 framework for reconstructing prehistoric human activity in obsidian. J. of the Fac. of
524 Sci. Univ. of Tokyo Sec. V Anthropol. IV-1, 241-317.
525 Tripcevich, N., Eerkens, J.W., Carpenter, T.R., 2012. Obsidian hydration at high
526 elevation: archaic quarrying at the Chivay source, southern Peru. J. Archaeol. Sci. 39,
527 1360-1367.
528 VanPool, T.L., Leonard, R.D., 2011. Quantitative Analysis in Archaeology. Willey-
529 Blackwell, West Sussex.
530 Watanabe, K., Suzuki, M., 2006. A relationship between hydration rate and chemical
531 composition of obsidian. Archaeol. and Nat. Sci. (Kokogaku to Shizenkagaku) 54, 1-12.
532 (in Japanese)
533 Yokoyama, Y., Kido, Y., Tada, R., Miniami, I., Finkel, R.C., Matsuzaki, H. 2007. Japan
534 Sea oxygen isotope stratigraphy and global sea-level changes for the last 50,000 years
535 recorded in sediment cores from the Oki Ridge. Paleogeography, Paleoclimatology,
536 Palaeoecol. 247, 5-17.
537 Yuan, D., Cheng, H., Edwards, R.L., Dykoski, C.A., Kelly, M.J., Zang, M., Qing, J.,

538 Lin, Y., Wang, Y., Wu, J., Dorale, J.A., An, Z., Cai, Y., 2004. Timing, duration, and
539 transitions of the Last interglacial Asian Monsoon. Science 304, 575-578.
540 Yurimoto, H., Nagashima, K., 2005. Development of isotope-microscopy and
541 implications for cosmochemistry. Microsc. Microanal. 11 (Suppl. 2), 196-197.
542 Yurimoto, H., Nakashima, K., Kunihiro, T., 2003. High precision isotope-imaging of
543 materials. Appl. Surf. Sci. 203-204, 793-797.
544 Zhang, Y., Belcher, R., Ihinger, P.D., Wang, L., Xu, Z., Newman, S., 1997. New
545 calibration of infrared measurement of dissolved water in rhyolitic glasses. Geochem.
546 Cosmochim. Acta 61, 3089-3100.

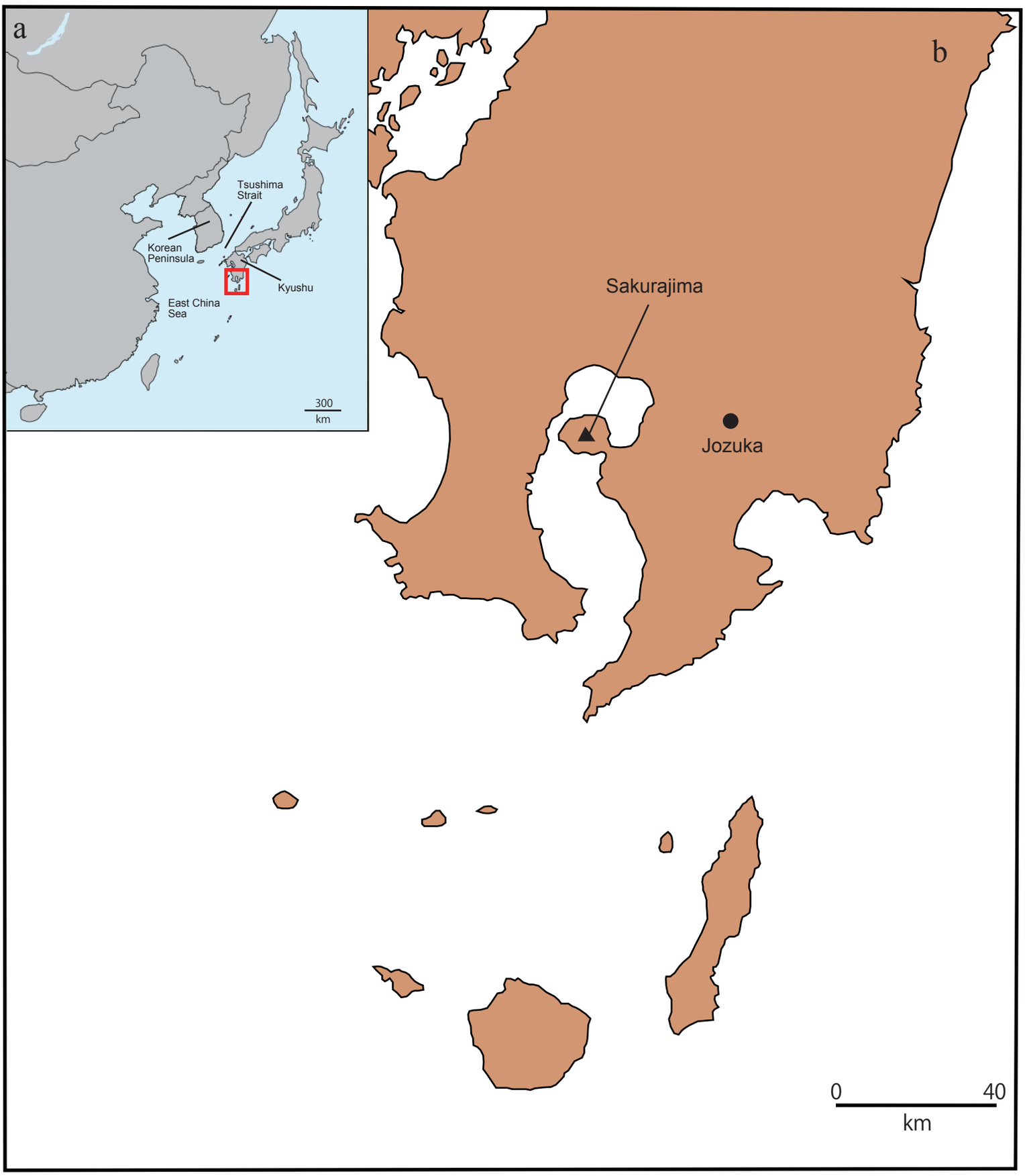
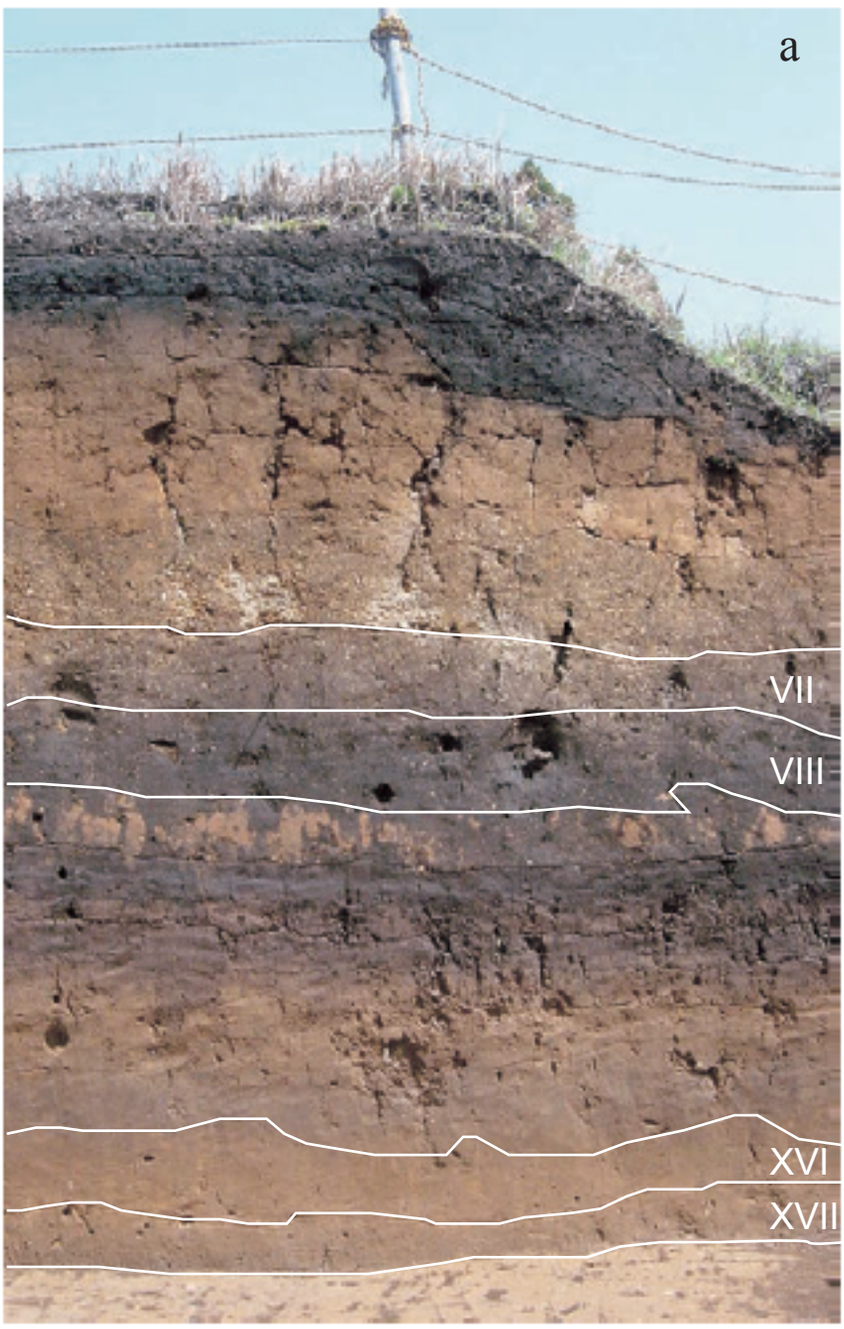

a
Tsushima
Strait
Korean
Peninsula
Kyushu
East China
Sea
300
km
b
Sakurajima
Jozuka
0
40
km

Figure 1


a
VII
VIII
XVI
XVII
0
0.5 m

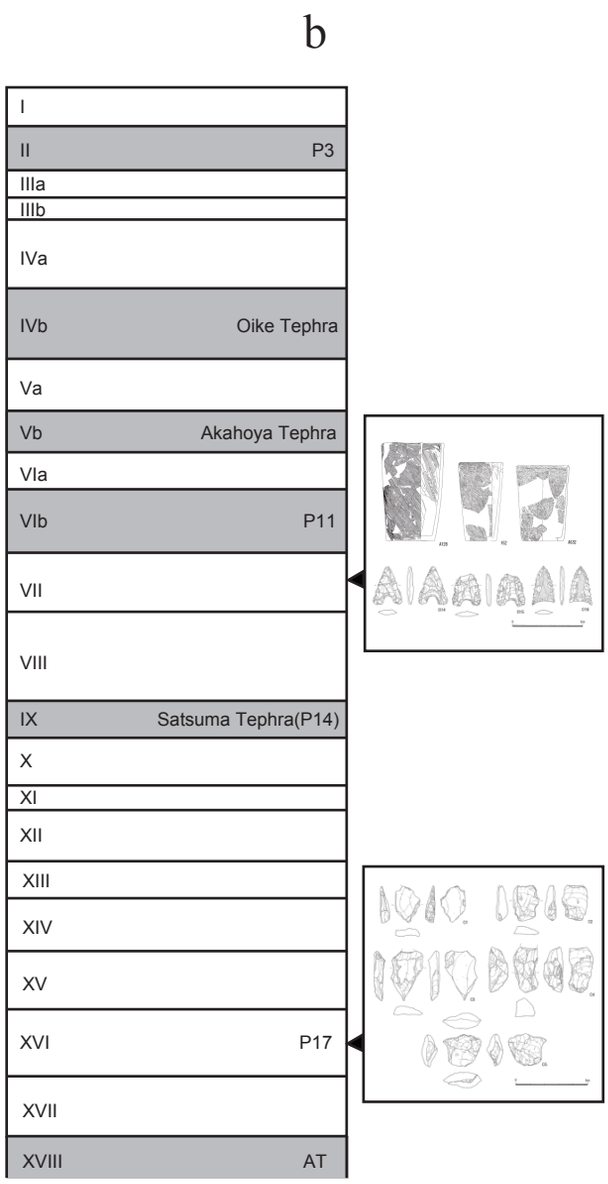

b
I
II
P3
IIIa
IIIb
IVa
IVb
Oike Tephra
Va
Vb
Akahoya Tephra
VIa
VIb
P11
VII
VIII
IX
Satsuma Tephra(P14)
X
XI
XII
XIII
XIV
XV
XVI
P17
XVII
XVIII
AT

Figure 2

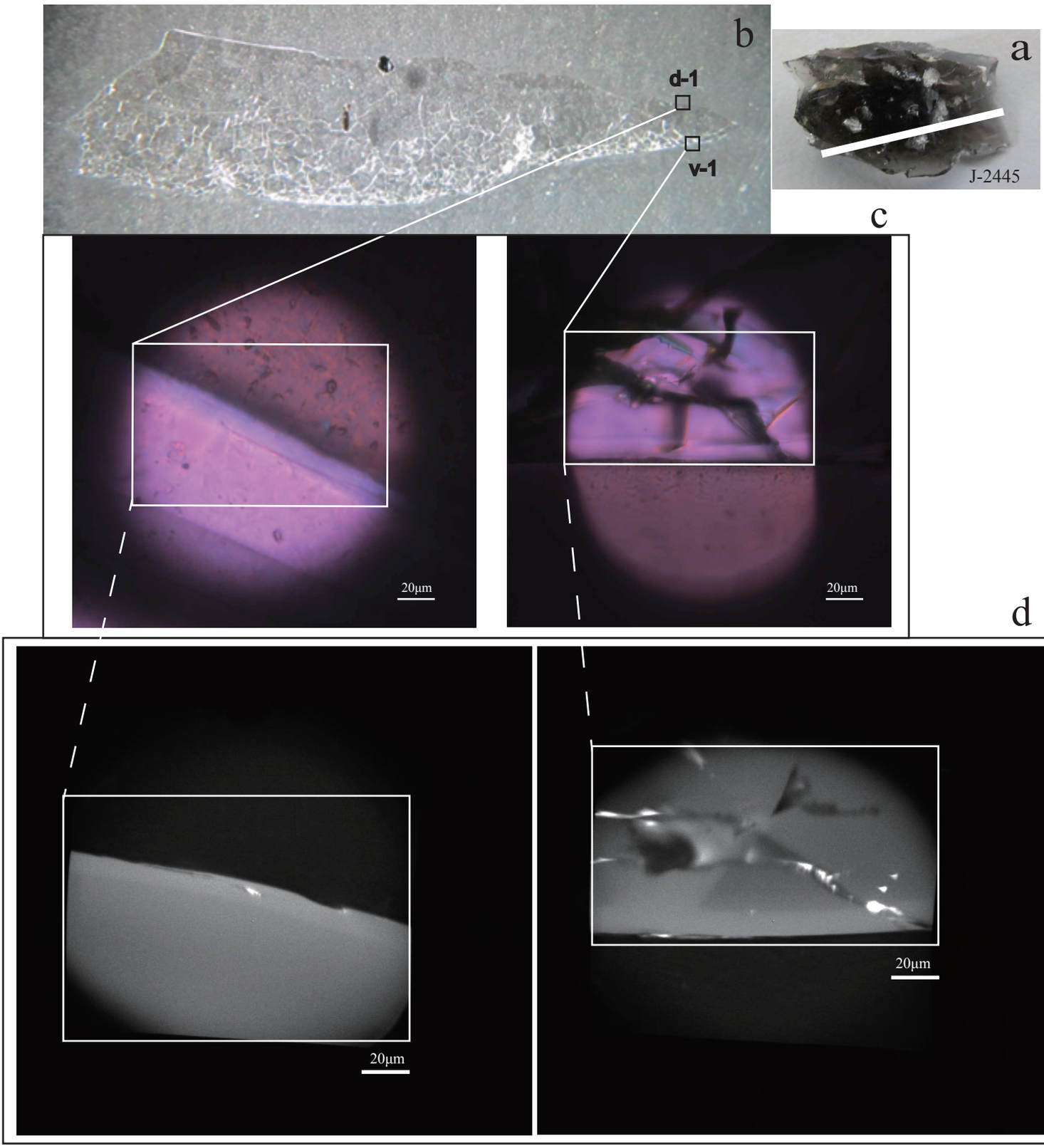


Figure 3

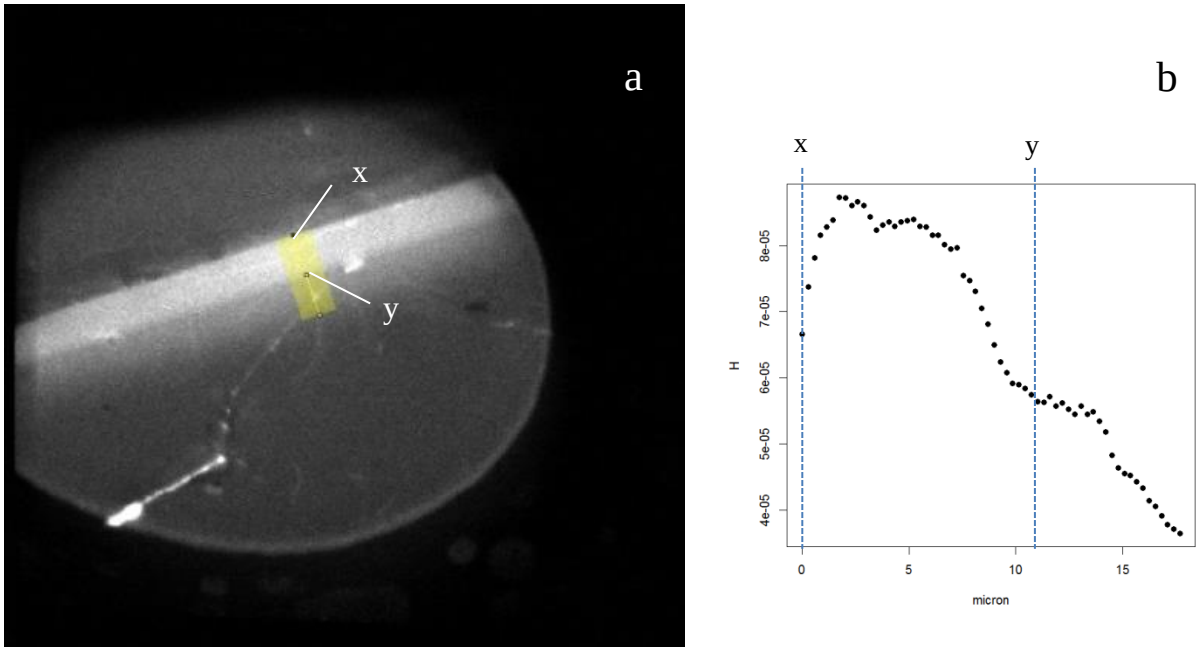


Figure 4

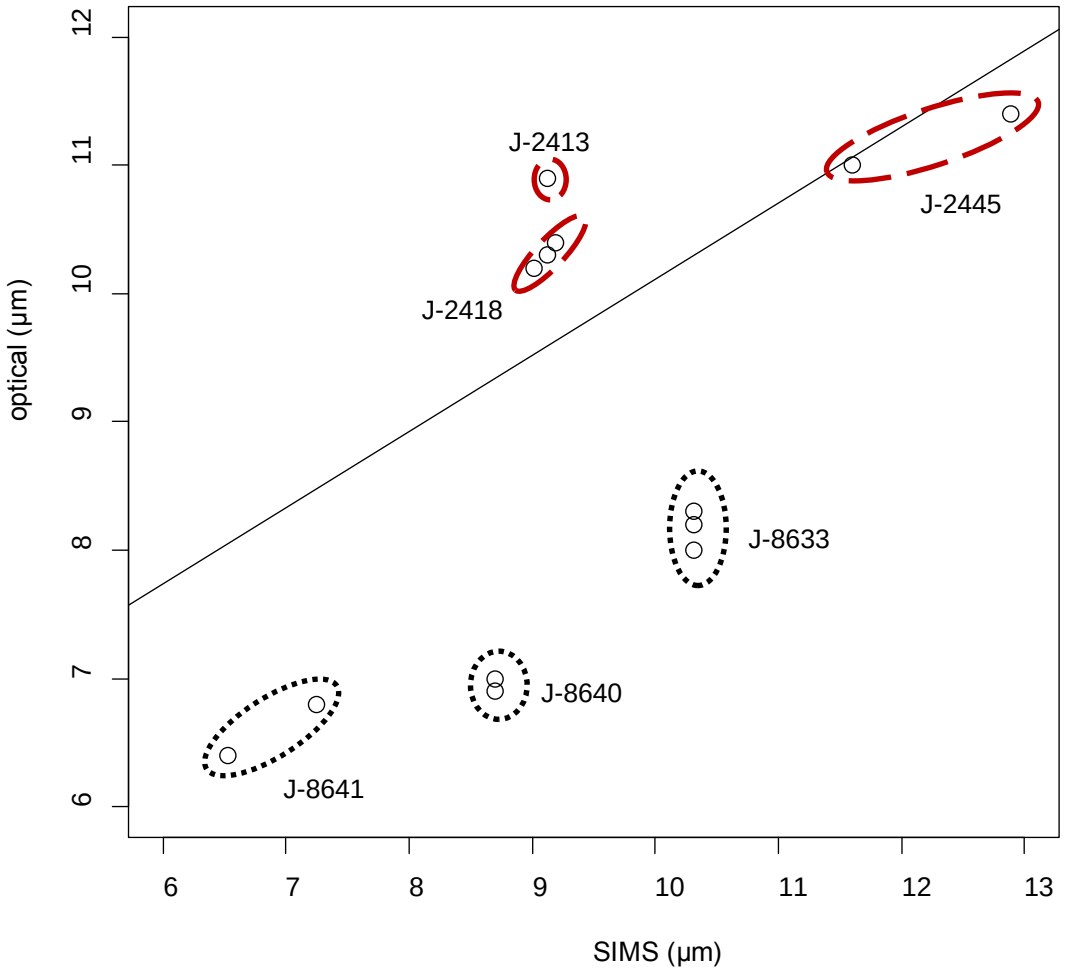

optical (μm)
SIMS (μm)
6
7
8
9
10
11
12
13
J-2413
J-2418
J-2445
J-8633
J-8640
J-8641
Measurements taken from an identical obsidian flake
Upper Paleolithic levels (ca. 26 ka)
Initial Jomon levels (ca. 10.5 ka)

Figure 5

Laboratory Number	Material Dated	Level	Associated features and artifacts	^{14}C Age BP	cal. B.P.
IAAA-82108	Charcoal	VII/VIII	Cobble concentration (#35)	8820±50	10155-9686
PLD-11056	Charred surface deposit	VII/VIII	Pottery	8875±35	10175-9793
IAAA-82106	Charcoal	VII/VIII	Pit-house (SH16)	8910±50	10204-9795
PLD-11055	Charred surface deposit	VII/VIII	Pottery	9195±40	10491-10247
IAAA-80833	Charcoal	VII/VIII	Pit-house (SH22)	9210±40	10496-10252
PLD-11054	Charred surface deposit	VII/VIII	Pottery	9220±40	10501-10258
IAAA-82107	Charcoal	VII/VIII	Cobble concentration (#25)	9310±40	10654-10303
IAAA-80835	Charcoal	VII/VIII	Pit-house (SH62)	9420±40	10752-10561
IAAA-80836	Charcoal	VII/VIII	Pit	9480±40	11068-10586
IAAA-82105	Charcoal	VII/VIII	Pit-house (SH04)	9480±40	11068-10586
PLD-11051	Charred surface deposit	VII/VIII	Pottery	9500±35	11070-10608
IAAA-80834	Charcoal	VII/VIII	Pit-house (SH31)	9500±40	11072-10605
PLD-11052	Charred surface deposit	VII/VIII	Pottery	9540±35	11081-10709
PLD-11053	Charred surface deposit	VII/VIII	Pottery	9750±35	11238-11136

Table 1. ^{14}C Dates from Levels VII and VIII (Initial Jomon occupation).

Sample	Age	A: microscopic thickness (μm) by optical microscope	B: hydrogen depth (μm) by SIMS	A - B	An evaluation of optical measurements
J-2413-d-3	26.5 ka	10.9	9.12	1.78	overestimate
J-2418-v-1	26.5 ka	10.4	9.19	1.21	overestimate
J-2418-v-2	26.5 ka	10.3	9.12	1.18	
J-2418-v-3	26.5 ka	10.2	9.02	1.18	
J-2445-d-1	26.5 ka	11	11.6	-0.6	underestimate
J-2445-v-1	26.5 ka	11.4	12.89	-1.49	
J-8633-d-3	10.5 ka	8.2	10.31	-2.11	underestimate
J-8633-v-1	10.5 ka	8	10.31	-2.31	
J-8633-v-2	10.5 ka	8.3	10.31	-2.01	
J-8640-d-3	10.5 ka	6.9	8.7	-1.8	underestimate
J-8640-v-2	10.5 ka	7	8.7	-1.7	
J-8641-d-2	10.5 ka	6.4	6.53	-0.13	underestimate
J-8641-v-2	10.5 ka	6.8	7.25	-0.45	

Table 2. Optical thickness compared with hydrogen depths, with an evaluation of microscopic measurements relative to hydrogen depths. Optical measurements and hydrogen depths are correlated at 5% level (Pearson's $r = 0.65$, $p = 0.016$).

Captions of figures and tables

Figure 1. Locations of southern Kyushu, the Jozuka site, and the related geographic locations. a: Map of Southeast Asia and the squared area is the southern Kyushu, b: southern Kyushu. Map of a is extracted from Wikimedia commons (https://commons.wikimedia.org/wiki/File:East_Asia_area_blank_CJK.svg)

Figure 2. Stratigraphic profile of the Jozuka, southern Kyushu. a: profile picture (from Kagoshima Prefectural Archaeological Center, 2010), b: schematic stratigraphic sequence. Shaded layers are pumice deposits. Obsidian flakes were sampled from Levels XVI and VII.

Figure 3. Optical hydration rims and corresponding micro-images of hydrogen on obsidian artifact (sample # J-2445). White line on obsidian flake (a) is at the location where thin section (b) was made. d-1 is a spot of measurement on ventral surface, and v-1 is that of ventral surface. (c) optical rim images. (d) micro-imaging.

Figure 4. (a) Micro-image of the hydrated surface, (b) SIMS hydrogen profile. x: at surface of obsidian. y: spot where hydrogen diminishes to background. Sample number is J-2413-d-3.

Figure 5. Plot of optical rim thicknesses against hydrogen depths (μm).

Table 1. ^{14}C Dates from Levels VII and VIII (Initial Jomon occupation).

Table 2. Measurements and related statistics for the samples from Jozuka site.

Note: The standard residual is calculated by the following equation: $SR = \frac{d_{Y*X}}{S_{Y*X}\sqrt{(1-h_i)}}$

where d_{Y*X} is raw residuals given as Y_i - $\hat{Y}$ as described above, hi is the leverage coefficient given as $h_i = \frac{1}{n} + \frac{(X_i - \hat{X})^2}{\sum x^2}$, S_{Y*X} is the mean square error given as $\sum_{i=1}^{n} \frac{(Y_i - \hat{Y})^2}{n-2}$